Magnetic anisotropy in thin films of Prussian blue analogues

D. M. Pajerowski,[1] J. E. Gardner,[2] M. J. Andrus,[2] S. Datta,[3] A. Gomez,[4] S. W. Kycia,[4] S. Hill,[3]
D. R. Talham,[2] and M. W. Meisel[1]
[1]*Department of Physics and the National High Magnetic Field Laboratory, University of Florida, Gainesville, Florida 32611-8440, USA*
[2]*Department of Chemistry, University of Florida, Gainesville, Florida 32611-7200, USA*
[3]*National High Magnetic Field Laboratory and Department of Physics, Florida State University, Tallahassee, Florida 32310-3706, USA*
[4]*Department of Physics, University of Guelph, Guelph, Ontario, Canada N1G 2W1*
(Received 7 October 2010; published 2 December 2010)

The magnetic anisotropy of thin (~200 nm) and thick (~2 μm) films and of polycrystalline (diameters ~60 nm) powders of the Prussian blue analogue $Rb_{0.7}Ni_{4.0}[Cr(CN)_6]_{2.9}\cdot nH_2O$, a ferromagnetic material with $T_c \sim 70$ K, have been investigated by magnetization, ESR at 50 and 116 GHz, and variable-temperature x-ray diffraction (XRD). The origin of the anisotropic magnetic response cannot be attributed to the direct influence of the solid support but the film growth protocol that preserves an organized two-dimensional film is important. In addition, the anisotropy does not arise from an anisotropic g tensor nor from magnetolattice variations above and below T_c. By considering effects due to magnetic domains and demagnetization factors, the analysis provides reasonable descriptions of the low- and high-field data, thereby identifying the origin of the magnetic anisotropy.

DOI: 10.1103/PhysRevB.82.214405 PACS number(s): 75.30.Gw, 68.37.Yz, 75.50.Xx, 76.30.−v

I. INTRODUCTION

There is an increasing demand for novel architectures that afford the possibility of spin-polarized electron transport, a field known as spintronics.[1] A key element involves control of the magnetic anisotropy in ferromagnetic films and nanostructures. Accordingly, the ability to manipulate the underlying magnetic states of the spin polarizers is desirable. In addition to traditional solid-state materials, molecule-based magnetic systems are being investigated.[2–4] The discovery of large and persistent photoinduced changes in the magnetization in some examples of cyanometallate coordination polymers makes them attractive materials to consider.[5,6]

Herein, studies of the magnetic anisotropy of thin and thick films along with standard powderlike samples of bimetallic Prussian blue analogues, $A_jM'_k[M(CN)_6]_\ell\cdot nH_2O$, where A is an alkali ion and M' and M are transition-metal ions,[7,8] are reported. Previously, the anisotropic response of the persistent photoinduced magnetism of thin films of Rb-Co-Fe (referring to A-M'-M) Prussian blue analogues was discovered[9] and subsequently studied systematically.[10–15] The motivation to understand the origins of this anisotropic phenomenon is amplified by the ability to control the magnetization of Prussian blue analogues by photoirradiation[5,6,16] or pressure.[17] However, the magnetic response of the photocontrollable A-Co-Fe system is complicated by the multiple stable oxidation states of the Co and Fe ions and by orbital angular momentum contributions. Consequently, the Rb-Ni-Cr Prussian blue analogue, a ferromagnet system possessing a spectrum of long-range ordering temperatures, $T_c \sim 60-90$ K, depending on stoichiometry,[8] was chosen as the centerpiece for the present work because the magnetic and physical properties of this system are robust and the ions have stable oxidation states that possess no first-order angular momentum.

Finally, it is important to stress the significance of our findings. Although the study of the magnetism of solid-state films is a mature field, the extensions to molecule-based magnetism are just beginning to emerge. For example, with the drive to develop new devices, applications with single crystals are being explored.[18] However, the exploitation of molecule-based magnetic films may be more attractive for industrial fabrication, and devices based on metal-phthalocyanines[19] and metal-[TCNE: tetracyanoethylene]$_x$ (Ref. 20) are two examples of work in this direction. In our work, the origins of the magnetic anisotropy in films of Prussian blue analogues will be linked to demagnetization effects after we have systematically eliminated all other plausible explanations, some of which are not issues in traditional solid-state magnetic films. As a result, our results provide a foundation from which the magnetism in films of Prussian blue analogues may be understood and employed in new devices.

II. EXPERIMENTAL DETAILS

The synthesis of the powder samples followed established protocols[14] while the films were generated using sequential adsorption methods[21] that are detailed elsewhere.[14] Briefly stated, the film synthesis consists of using a solid support, such as Melinex 535, and immersing it in an aqueous solution of Ni^{2+} ions and then in another aqueous solution of $Cr(CN)_6^{3-}$ containing Rb^+ ions. After each immersion step, washing with water is essential to remove the excess ions, and the process can be iterated multiple cycles to yield films of varying thicknesses and morphologies. For this work, two films, one of 40 cycles and the other of 400 cycles, are reported. Whereas the powder samples consisted of small polycrystals with diameters of ~60 nm, which are magnetically in the "bulk" limit,[22] the 40 cycles and 400 cycles films had thicknesses of ~200 nm and ~2 μm, respectively. Finally, other Rb-M'-M Prussian blue analogue films were investigated, including Rb-Co-Cr, Rb-Cu-Cr, Rb-Zn-Cr, Rb-Ni-Fe, Rb-Co-Fe, Rb-Cu-Fe, and Rb-Zn-Fe.[14,15]

The chemical compositions and the physical properties of all samples were established by a suite of techniques, which yielded $Rb_{0.7}Ni_{4.0}[Cr(CN)_6]_{2.9}\cdot nH_2O$.[14,15] For the magnetization measurements, a commercial (Quantum Design) magnetometer was used in conjunction with a homemade *in situ* rotator.[23] The powder samples were mounted in gelcaps while the film samples were either cut and stacked in a plastic box or measured individually in a straw holder. A single 400 cycles film, a stack of ten 40 cycles films, and ~100 μg of powder embedded in eicosane were employed for the cw-electron spin resonance (ESR) measurements performed at either 50 or 116 GHz, using a resonant cavity coupled to a cryostat and superconducting magnet at the NHMFL-Tallahassee.[24] Transmission and reflection x-ray diffraction (XRD) studies were performed at 20, 110, and 300 K by using the instruments at the University of Guelph. Care was taken to avoid long-term vacuum pumping of the sample at room temperature since variations due to reversible dehydration-hydration[25,26] were observed as the (200) peak shifted to higher 2θ and broadened. Data were collected for nominally 24 h at each temperature, and a blank Melinex film was also measured to assist with the background subtraction arising from the solid support.

III. RESULTS

The anisotropic magnetic response in Prussian blue analogues was initially observed in magnetization measurements,[9] and this behavior is shown for the Rb-Ni-Cr films in Figs. 1 and 2. Differences between the zero-field-cooled (ZFC) and field-cooled (FC) data are related to a spin-glass-like response,[27,28] while the anisotropy of the thin and thick films is strikingly similar as the external magnetic field is applied parallel or perpendicular to the surface of the films, hereafter referred to as $B\parallel$ and $B\perp$, respectively. This behavior is also present, albeit to a somewhat weaker degree, in spin-cast samples[14] but is not observed in films that were synthesized in a manner that corrupts their two-dimensional nature by generating discontinuities and roughness.[10]

To date, ESR investigations of Prussian blue analogues have been limited to the Rb-Mn-Fe system that ferromagnetically orders near 10 K.[29,30] In our work, the nature of the anisotropy was explored, and the 116 GHz results for the powder and 2 μm film are shown in Fig. 3, while the data for the 200 nm film are consistent with the trends reflected in the thicker film.[15] One difference is that the lines of the thin film have a Lorentzian shape while the lines of the thick film have a Gaussian shape, and this observation is consistent with the increase in disorder as the films become thicker. For the powder, one clear absorption line, with an effective $g=2.05$, is resolved. The response of the 2 μm film is similar to the powder for $T\gtrsim 100$ K for both orientations of the applied magnetic field. However, for $T<100$ K, the absorption signals are described by two lines, one main line that is temperature dependent and a weak line that is independent of temperature within experimental resolution. Whereas the main line presumably arises from the well coupled Ni^{2+} and Cr^{3+} ions, the weak line is associated with trace amounts of powder-sized nodules that are observed on the surfaces of the films.[14,15]

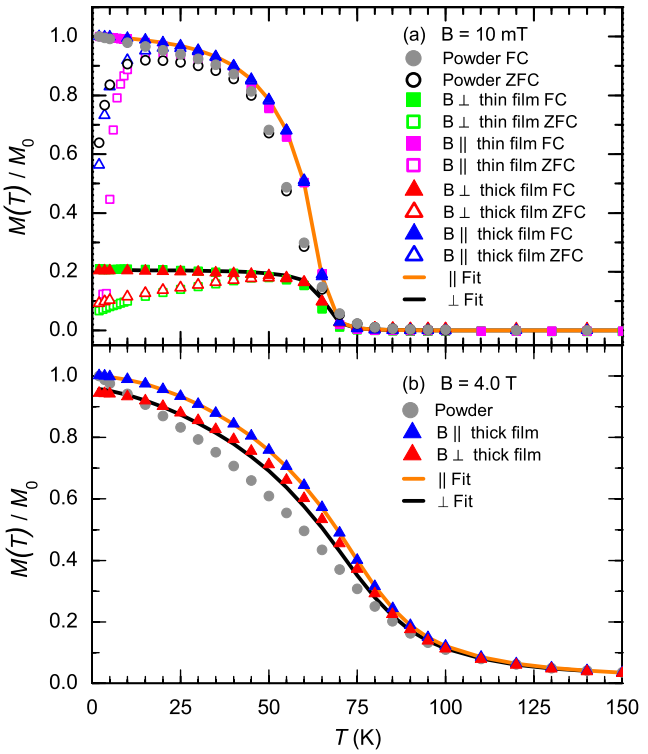

FIG. 1. (Color online) The temperature dependences of the ZFC and FC magnetizations, $M(T)$, normalized to the FC values at $T=2$ K, M_0, are shown for (a) low, $B=10$ mT, and (b) high, $B=4$ T, applied magnetic fields. For clarity, the data for the thin film are not shown in (b). The anisotropic response for B applied parallel ($\parallel$) or perpendicular ($\perp$) to the films is strikingly similar for both thin and thick films. The field-induced shift of T_c from ~70 to ~100 K is observable. For each panel, the solid lines are the results of analysis using demagnetization factors (see text).

At 10 K, the main and weak lines have effective g values of 2.11 and 2.05 for $B\parallel$ and 1.97 and 2.05 for $B\perp$. The temperature dependences of the main line positions are shown in Fig. 4, along with the angular dependences of the main and weak lines at 50 and 116 GHz for the 2 μm film at

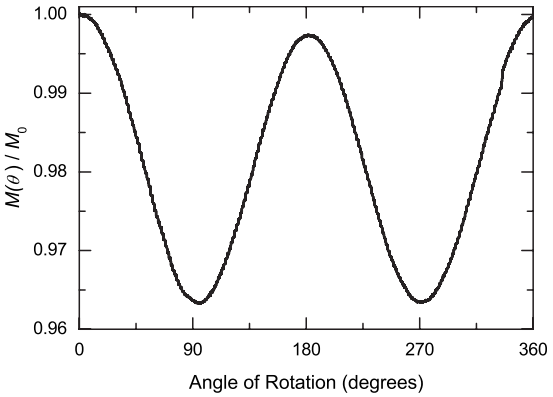

FIG. 2. The angular variation in M is shown for the case of the thick film when $B=4$ T and $T=10$ K. The discrete steps of 1.5° are detectable, and the data were taken continuously at each angle that was held for a period of 5 min. The data for the thin film and additional details are available elsewhere (Ref. 15).

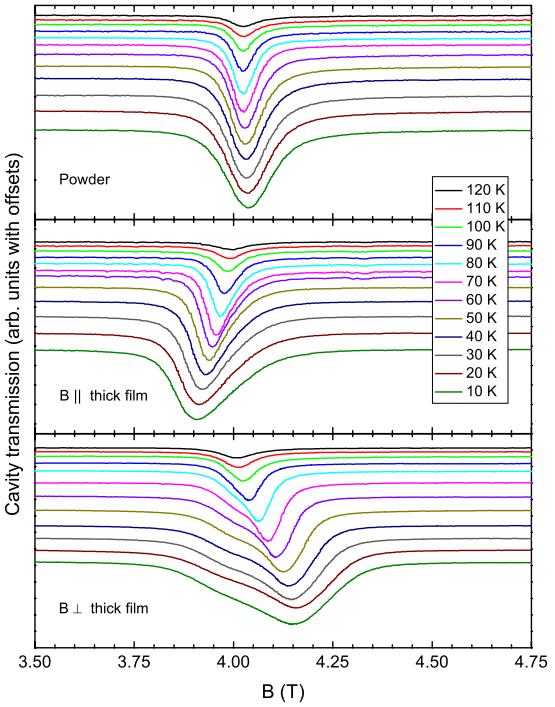

FIG. 3. (Color online) The cavity transmission at 116 GHz, as a function of B, is shown for various temperatures for the powder and the thick (2 μm) film for $B \parallel$ and $\perp$ to the surface of the film. The traces are offset for clarity.

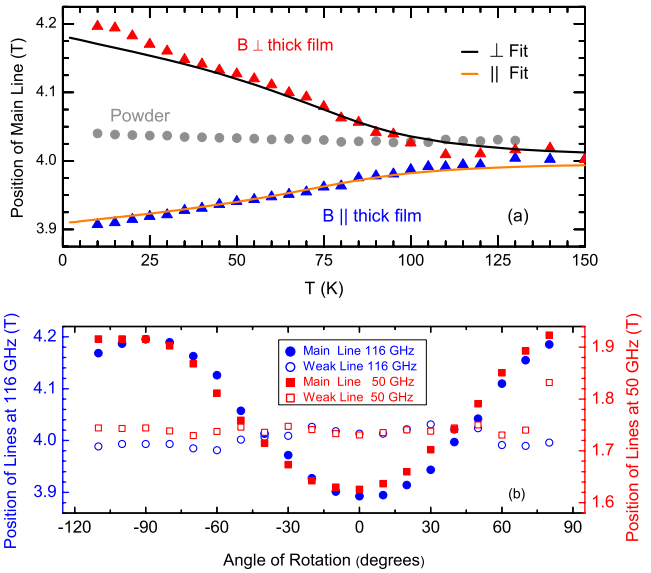

FIG. 4. (Color online) (a) The temperature dependences of the main ESR absorption lines at 116 GHz (Fig. 3), for the powder specimen and the thick film with $B \parallel$ and $\perp$ to the surface of the film. The solid lines are the results of analysis using demagnetization factors, see text. (b) Angular dependences of the positions of the main (closed symbols) and weak (open symbols) ESR absorption lines at 116 GHz (round symbols and left scale) and at 50 GHz (square symbols and right scale). The $B \parallel$ and $\perp$ orientations are 0° and ±90°, respectively.

10 K. The angular response of the main line is identical to the behavior observed for the magnetization, Fig. 2, and follows a uniaxial $\sin^2(\alpha)$ dependence, where α is the angle between B and the surface of the film. In addition, the angular dependence of the positions of the main lines is the same at both frequencies with a maximum variation of $\Delta B \sim 0.3$ T (Fig. 4).

Since deviations from perfect cubic symmetry[31] might arise when the samples cool through T_c, variable temperature XRD studies were performed (Fig. 5). The (200) and (400) peaks at 17.16° and 34.68° were monitored in detail, and the results do not indicate any change in the lattice parameter through T_c, as the $Fm\bar{3}m$ (No. 225) cubic symmetry is maintained with a lattice dimension of 10.33 Å. In transmission, the peaks at 24° and 30° were also assignable due to the absence of contributions from the polymer solid support in this configuration.

IV. DISCUSSION

After inspecting the comprehensive set of experimental results, several points are immediately obvious. First and simply stated, the films possess magnetic anisotropy that is not manifested in polycrystalline powder samples that are normally studied. Second, the data indicate that the underlying anisotropy prevails for thin and thick films, so the anisotropy does not explicitly arise from influences coming from direct interaction with the solid support[32] but does depend upon the two-dimensional organization of the sample generated during the film fabrication process. Furthermore, the values of T_c are independent of the orientation of the magnetic field, meaning the anisotropy does not originate from variations in the superexchange parameter, J. Third, the ESR results, namely, the line shapes of the powder spectra and the frequency independence of the magnitude of the line splittings, cannot be reconciled by the presence of an anisotropic g tensor. Finally, magnetostriction or other structural changes are not observed at any temperature, so the cubic symmetry is preserved to an extent that does not permit it to be a possible explanation of the anisotropy.

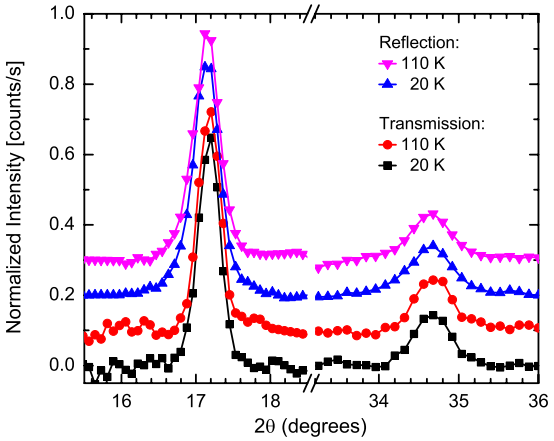

FIG. 5. (Color online) The XRD pattern collected in reflection and transmission modes at 20 and 110 K. The results near the (200) and (400) peaks are shown when normalized to the peak values of each data set. The data traces are shifted for clarity. No changes in the lattice parameters are detected to within 0.005 Å.

With the elimination of several common mechanisms as the possible sources of the anisotropic response, magnetostatic interactions remain as a plausible explanation. Indeed, the uniaxial nature of the anisotropy is consistent with dipolar interactions. In addition, demagnetizing effects ($H_{\text{effective}}=H_{\text{lab}}-NM$, where N is the demagnetizing factor) model the data well when using the theoretical value to normalize the high-field, saturation magnetization value of 1.47×10^5 A/m, namely, $\langle S_{\text{Ni}_z}\rangle_{\max}=1$ and $\langle S_{\text{Cr}_z}\rangle_{\max}=3/2$.[15,33,34] The low-field magnetization in the perpendicular orientation can be reproduced quantitatively from the parallel orientation if $N_{\parallel}=0.07$ and $N_{\perp}=0.86$, Fig. 1(a), where domains are expected to obey $2N_{\parallel}+N_{\perp}=1$.[33,34] The high-field magnetization can also be reproduced but not as directly since the high-field susceptibility has a significant experimental uncertainty because dM/dH is orders of magnitude smaller than M/H in this range. Nevertheless, the uniformly magnetized film limit, *vide infra*, namely, $N_{\parallel}=0$ and $N_{\perp}=1$, reasonably reproduces the observed trends [Fig. 1(b)].

The ESR data can also be explained by the presence of demagnetization effects.[34–36] Specifically, taking the equations of motion for a spin in B along the z axis, the resonance condition is

$$\omega_0^2=g^2\mu_B^2[B_z+(N_y-N_z)\mu_o M_z][B_z+(N_x-N_z)\mu_o M_z]. \tag{1}$$

For a perfect sphere, $N_x=N_y=N_z=1/3$, so the resonance condition should be isotropic and have no magnetization dependence. In practice, there may be small deviations from spherical symmetry for the powder, and the resonance condition may be written as

$$\omega_{0,\text{powder}}=g\mu_B[B-\mu_o\delta M_z], \tag{2}$$

where δ takes care of deviations from spherical symmetry. For the powder data, Figs. 2 and 3, a shift of $\sim$10 mT is present in the fully magnetized state compared to the paramagnetic state. This observation is consistent with a value of $\delta\sim0.05$, and the shift is similar to the one reported for Rb-Mn-Fe,[29] where it was attributed to demagnetizing effects. For a uniformly magnetized film oriented perpendicular to B, the resonance condition is

$$\omega_{0,\perp}=g\mu_B[B-\mu_o M_z], \tag{3}$$

whereas for the parallel orientation, the resonance condition is

$$\omega_{0,\parallel}=g\mu_B[B(B+\mu_o M_z)]^{1/2}. \tag{4}$$

Ergo, the temperature dependence of the main lines can be predicted with $N_{\parallel}=0$ and $N_{\perp}=1$, and the results are in excellent agreement with the data [Fig. 4(a)].

V. CONCLUSIONS

In summary, the observed magnetic anisotropy of the Rb-Ni-Cr Prussian blue analogue films is attributable to demagnetization effects arising from their two-dimensional geometry. Additional evidence for the magnetic domain-field interactions is garnered from the extensive data sets collected on the aforementioned Rb-M'-M Prussian blue analogues.[14,15] Having identified magnetic domains as the origin of the anisotropy, additional studies, such as magnetic imaging of the surfaces, will provide a deeper understanding of the architecture and dynamics of the domains. Finally, a systematic approach for determining the nature of magnetic anisotropy in coordination polymers has been presented and will be important as this class of materials is investigated for physical properties applicable to spintronic applications.

ACKNOWLEDGMENTS

We acknowledge conversations with M. F. Dumont, M. W. Lufaso, and A. Ozarowski. This work was supported, in part, by NSERC, CFI, and NSF through Grants No. DMR-0804408 (S.H.), No. DMR-1005581 (D.R.T.), and No. DMR-0701400 (M.W.M.), and the NHMFL via cooperative agreement under NSF Grant No. DMR-0654118 and the State of Florida. We thank Ben Pletcher and the Major Analytical Instrumentation Center (MAIC), Department of Materials Science and Engineering, University of Florida, for help with the EDS, SEM, and TEM work.

[1] S. A. Wolf, D. D. Awschalom, R. A. Buhrman, J. M. Daughton, S. von Molnár, M. L. Roukes, A. Y. Chtchelkanova, and D. M. Treger, Science **294**, 1488 (2001).
[2] L. Bogani and W. Wernsdorfer, Nature Mater. **7**, 179 (2008).
[3] J. Camarero and E. Coronado, J. Mater. Chem. **19**, 1678 (2009).
[4] Y. Moritomo and T. Shibata, Appl. Phys. Lett. **94**, 043502 (2009).
[5] O. Sato, T. Iyoda, A. Fujishima, and K. Hashimoto, Science **272**, 704 (1996).
[6] D. M. Pajerowski, M. J. Andrus, J. E. Gardner, E. S. Knowles, M. W. Meisel, and D. R. Talham, J. Am. Chem. Soc. **132**, 4058 (2010).
[7] K. R. Dunbar and R. A. Heitz, Prog. Inorg. Chem. **45**, 283 (1997).
[8] M. Verdaguer and G. S. Girolami, in *Magnetism: Molecules to Materials V*, edited by J. S. Miller and M. Drillon (Wiley-VCH, Weinheim, Germany, 2005), p. 283.
[9] J.-H. Park, E. Čižmár, M. W. Meisel, Y. D. Huh, F. Frye, S. Lane, and D. R. Talham, Appl. Phys. Lett. **85**, 3797 (2004).
[10] J.-H. Park, F. Frye, S. Lane, Y. D. Huh, E. Čižmár, D. R. Talham, and M. W. Meisel, Polyhedron **24**, 2355 (2005).
[11] F. A. Frye, D. M. Pajerowski, J.-H. Park, M. W. Meisel, and D. R. Talham, Chem. Mater. **20**, 5706 (2008).
[12] J.-H. Park, Ph.D. thesis, University of Florida, 2006.
[13] F. A. Frye, Ph.D. thesis, University of Florida, 2007.
[14] J. E. Gardner, Ph.D. thesis, University of Florida, 2009.
[15] D. M. Pajerowski, Ph.D. thesis, University of Florida, 2010.
[16] A. Bleuzen, C. Lomenech, V. Escax, F. Villain, F. Varret, C.

Cartier dit Moulin, and M. Verdaguer, J. Am. Chem. Soc. **122**, 6648 (2000).
[17] M. Zentková, Z. Arnold, J. Kamarád, V. Kavečanský, M. Lukáčová, S. Mat'aš, M. Mihalik, Z. Mitróová, and A. Zentko, J. Phys.: Condens. Matter **19**, 266217 (2007).
[18] R. D. Schmidt, D. A. Shultz, J. D. Martin, and P. D. Boyle, J. Am. Chem. Soc. **132**, 6261 (2010).
[19] S. Heutz, C. Mitra, W. Wu, A. J. Fisher, A. Kerridge, M. Stoneham, A. H. Harker, J. Gardener, H.-H. Tseng, T. S. Jones, C. Renner, and G. Aeppli, Adv. Mater. **19**, 3618 (2007).
[20] J.-W. Yoo, C.-Y. Chen, H. W. Jang, C. W. Bark, V. N. Prigodin, C. B. Eom, and A. J. Epstein, Nature Mater. **9**, 638 (2010).
[21] J. T. Culp, J.-H. Park, I. O. Benitez, Y. D. Huh, M. W. Meisel, and D. R. Talham, Chem. Mater. **15**, 3431 (2003).
[22] D. M. Pajerowski, F. A. Frye, D. R. Talham, and M. W. Meisel, New J. Phys. **9**, 222 (2007).
[23] D. M. Pajerowski, and M. W. Meisel, J. Phys.: Conf. Ser. **150**, 012034 (2009).
[24] S. Takahashi and S. Hill, Rev. Sci. Instrum. **76**, 023114 (2005).
[25] S. Ohkoshi, K. Arai, Y. Sato, and K. Hashimoto, Nature Mater. **3**, 857 (2004).
[26] Y. Moritomo, F. Nakada, J. Kim, and M. Takata, Appl. Phys. Express **1**, 111301 (2008).
[27] D. A. Pejaković, J. L. Manson, J. S. Miller, and A. J. Epstein, Phys. Rev. Lett. **85**, 1994 (2000).
[28] J. A. Mydosh, *Spin Glasses* (Taylor & Francis, London, 1993).
[29] M. Pregelj, A. Zorko, D. Arčon, S. Margadonna, K. Prassides, H. van Tol, L. C. Brunel, and O. Ozarowski, J. Magn. Magn. Mater. **316**, e680 (2007).
[30] Á. Antal, A. Jánossy, L. Forró, E. J. M. Vertelman, P. J. van Koningsbruggen, and P. H. M. van Loosdrecht, Phys. Rev. B **82**, 014422 (2010).
[31] A. Bleuzen, J.-D. Cafun, A. Bachschmidt, M. Verdaguer, P. Münsch, F. Baudelet, and J.-P. Itié, J. Phys. Chem. C **112**, 17709 (2008).
[32] P. Gambardella, S. Stepanow, A. Dmitriev, J. Honolka, F. M. F. de Groot, M. Lingenfelder, S. S. Gupta, D. D. Sarma, P. Bencok, S. Stanescu, S. Clair, S. Pons, N. Lin, A. P. Seitsonen, H. Brune, J. V. Barth, and K. Kern, Nature Mater. **8**, 189 (2009).
[33] J. A. Osborn, Phys. Rev. **67**, 351 (1945).
[34] S. V. Vonsovskii, *Ferromagnetic Resonance* (Pergamon Press, Oxford, 1966).
[35] C. Kittel, *Introduction to Solid State Physics* (Wiley, New York, 1976).
[36] S. Kunii, J. Phys. Soc. Jpn. **69**, 3789 (2000).